

## ABSTRACT

KHOI NGUYEN

Exploring the HRP-Biosynthetic Pathway Through Two Fucosylation Mutations in *D. melanogaster*  
(Under the Direction of DR. MICHAEL TIEMEYER)

Anti-HRP staining of two *D. melanogaster* mutants generated from an ethyl methane sulfonate (EMS) mutagenesis, sugar-free frosting (*sff*) and MS16-2, revealed a decrease in embryonic HRP-epitope expression. MS16-2 embryos and  $w^{1118}$  embryos were prepared into protein powder and subsequently digested with peptide N-glycosidase (PNGase) F and A. The released glycans were analyzed with mass spectrometry. The N-glycan profile of both preparations showed similar glycan species and prevalence. The profiles also show a decrease in HRP-epitopes in MS16-2. Using [ $^{13}\text{C}$ ] methyl iodide and [ $^{12}\text{C}$ ] methyl iodide to differentially label glycans during permethylation, the relative abundance of N-linked glycans can be quantified and compared between  $w^{1118}$  and MS16-2 embryos.

Brains dissected from third-instar *sff* and  $w^{1118}$  larvae were prepared into protein powder and subsequently analyzed for N-glycans. The N-glycan profile of the *sff* larval brains showed a decrease in HRP-epitopes. Heads harvested from  $w^{1118}$ ,  $w^-$ ; *sff*, OreR, and  $w^+$ ; *sff* adult males were also analyzed for N-glycans. N-glycan analysis of the heads also showed a decrease in HRP-epitope expression in *sff* adult heads.

Geotaxis testing was performed on *sff* and MS16-2 adult males to examine the effects of the mutation. Wild type flies that go through geotaxis testing climb to the top of the vial within 15 seconds. Flies that were *sff*, however, displayed a less dynamic behavior, with the majority of flies staying in the vial. MS16-2 flies showed a similar behavior to *sff*, but not as severe as *sff*. The results of the geotaxis testing served as a basis for developing a geotaxis mutant screen. The screen could be used to isolate mutations that affect geotaxis behavior, with hopes of discovering mutations that affect different aspects of the HRP biosynthetic pathway.

INDEX WORDS: HRP-epitope, *Drosophila* Neural Development, *sff*, N-Glycan, Geotaxis, Fucosylation

EXPLORING THE HRP-BIOSYNTHETIC PATHWAY THROUGH TWO FUCOSYLATION  
MUTATIONS IN *DROSOPHILA MELANOGASTER*

by

KHOI NGUYEN

A Thesis Submitted to the Honors Council of the University of Georgia in Partial Fulfillment of  
the Requirements for the Degree

BACHELOR OF SCIENCE  
in BIOCHEMISTRY & MOLECULAR BIOLOGY  
with HIGHEST HONORS

Athens, Georgia

2008

EXPLORING THE HRP-BIOSYNTHETIC PATHWAY THROUGH TWO FUCOSYLATION  
MUTATIONS IN *DROSOPHILA MELANOGASTER*

by

KHOI NGUYEN

Approved:

Michael Tiemeyer  
Dr. Michael Tiemeyer  
Faculty Research Mentor

December 15, 2008  
Date

Approved:

Lance Wells  
Dr. Lance Wells  
Reader

December 15, 2008  
Date

Approved:

David S. Williams  
Dr. David S. Williams  
Director, Honors Program, Foundation Fellows and  
Center for Undergraduate Research Opportunities

December 17, 2008  
Date

Approved:

Pamela B. Kleiber  
Dr. Pamela B. Kleiber  
Associate Director, Honors Program and  
Center for Undergraduate Research Opportunities

December 17, 2008  
Date

## DEDICATION

I would like to dedicate this work to my parents, who have supported me through everything and have motivated me to do my best in life. I am the person I am today because of the teachings of my parents. I would also like to dedicate this work to everyone in Michael Tiemeyer's laboratory, especially Michael Tiemeyer and Mary Sharrow. They have graciously given me the opportunity to participate in a tremendous amount of research. I am grateful for their guidance and kindness in helping me in my undergraduate research experience.

## ACKNOWLEDGEMENTS

My deepest gratitude goes out to everyone in Michael Tiemeyer's laboratory. I would first like to thank Dr. Michael Tiemeyer, who gave me the opportunity to work in his laboratory and participate in numerous research projects. I would also like to thank Mary Sharrow, who has been a teacher and supervisor to me. She has helped me in almost everything I have done in the laboratory. I am also in gratitude of Kazuhiro Aoki and Mindy Porterfield, from whom I have learned everything I know about glycan analysis.

## TABLE OF CONTENTS

	Page
ACKNOWLEDGEMENTS .....	iv
LIST OF FIGURES .....	viii
CHAPTERS	
1 INTRODUCTION .....	1
N-Glycan Biosynthetic Pathway in Drosophila .....	1
The Role of Fucosylation in Drosophila Neural Development .....	2
Characterization of N-glycans in MS16-2 and sff Neural Tissues .....	3
2 MATERIALS AND METHODS .....	8
Drosophila Lines .....	8
Embryo, Larval Brains, and Adult Heads Collection .....	8
Glycan Preparation and Nanospray Ionization-Linear Ion Trap Mass Spectrometry .....	9
Geotaxis Testing .....	12
3 CHARACTERIZATION OF N-GLYCANS IN MS16-2 AND W <sup>1118</sup> EMBRYOS .....	15
Total N-Linked Glycan Profile of w <sup>1118</sup> and MS16-2 .....	15

	Release and Detection of Difucosylated Glycans .....	16
	Differential Isotopic Labeling of Glycans.....	16
	Possible Alterations in N-Glycan Biosynthesis Attributed to MS16-2 Mutation .....	17
4	N-GLYCAN EXPRESSION AT <i>sff</i> LARVAL AND ADULT STAGES .....	24
	N-glycan Profile of Larval <i>sff</i> and w <sup>1118</sup> Brains .....	24
	N-glycan Profile of Adult <i>sff</i> and Wild-Type Heads .....	24
	Speculations on <i>sff</i> Mutation and Comparison to MS16-2 Mutation .....	26
5	GEOTAXIS TESTING AND SCREENING .....	35
	Geotaxis Behavioral Test .....	35
	Development of Geotaxis Screen .....	35
	WORKS CITED .....	40

## LIST OF FIGURES

	Page
Figure 1: Pathway of N-glycan processing and modification .....	5
Figure 2: Detected HRP-epitopes in Drosophila embryo .....	5
Figure 3: Differentiation of neurons is driven by attenuation of Notch signaling and increased production of HRP-epitope .....	6
Figure 4: Dynamic relationship between O-linked fucosylation of Notch and N-linked fucosylation in signaling neural differentiation .....	7
Figure 5: Anti-HRP-epitope staining of $w^{1118}$ , MS16-2, and <i>sff</i> embryos .....	7
Figure 6: Tissue preparation and processing for glycan analysis .....	13
Figure 7: Release of N-glycans from protein powder .....	14
Figure 8: N-linked glycan profile released by PNGase A .....	19
Figure 9: N-glycan prevalence of $w^{1118}$ and MS16-2 embryos .....	20
Figure 10: Fragmentation pattern of M3N2F2 (mass = 1520) .....	21
Figure 11: Differential N-glycans profile of $w^{1118}$ and MS16-2 .....	22
Figure 12: Differentially labeled M3N2F2 peaks for $w^{1118}$ and MS16-2 .....	23
Figure 13: N-linked glycan profile of $w^{1118}$ and <i>sff</i> larval brains .....	29
Figure 14: N-glycan prevalence of $w^{1118}$ and <i>sff</i> larval brains .....	30
Figure 15: N-linked glycan profile of OreR and $w^+$ ; <i>sff</i> adult heads .....	31

Figure 16: N-glycan prevalence of OreR and $w^+$ ; <i>sff</i> adult heads .....	32
Figure 17: N-linked glycan profile of $w^{1118}$ and $w^+$ ; <i>sff</i> larval brains .....	33
Figure 18: N-glycan prevalence of $w^{1118}$ and $w^+$ ; <i>sff</i> adult heads .....	34
Figure 19: Geotaxis testing data for $w^{1118}$ , <i>sff</i> , and MS16-2 adult male flies .....	38
Figure 20: Steps in Geotaxis Screening .....	39

## CHAPTER 1 INTRODUCTION

Eukaryotic cells are enveloped by a complex facade of glycoproteins, glycolipids, and proteoglycans that constitute the interface at which cells interact with their environment and each other. Cell surface glycans mediate cellular recognition and adhesion, regulate protein activity, influence receptor ligation, and modulate transmembrane signaling (Seppo et al.). Specific glycan expression is essential for tissue development; oligosaccharide structures are the most distinctive markers for cellular differentiation in complex tissues. The cellular and molecular mechanisms by which cells achieve their unique cell surface glycans are largely unknown. As embryonic cells differentiate and form organized tissues, glycan expression diversifies, generating tissue- and cell-specific glycosylation profiles. The structural diversity of expressed glycans is determined by the expression and regulation of glycosyltransferase activities and by the availability of appropriate acceptor/donor substrates. Cells use these factors to generate unique glycan patterns in response to their environments.

### *N-Glycan Biosynthetic Pathway in Drosophila*

Biosynthesis of *N*-glycans in eukaryotes starts at the cytosolic face of the rough ER membrane, with the attachment of GlcNAc from UDP-GlcNAc to dolichol-P (Dol-P). The structure is expanded into Man<sub>5</sub>GlcNAc<sub>2</sub>, which is then transferred into the lumen of the rough ER. Additional glycosylation turns the oligosaccharide into the precursor molecule, Glc<sub>3</sub>Man<sub>9</sub>GlcNAc<sub>2</sub>, which becomes covalently attached to an asparagine residue of a

protein. The glucoses of the precursor are then trimmed one by one from the glycan in the ER. Glycan processing ensues in the ER and Golgi apparatus and several pathways are employed. Three destinies are possible for the high-mannose glycan: remain a high-mannose structure, become a pauci-mannose structure, or become a complex structure (Figure 1). The biosynthetic pathway of the pauci-mannose-type glycans may be stationed to interfere with the process to the complex-type glycans (Natsuka et al.). The pathway can be regarded as a route which leads to monotonous structures and hinders diverse formation of glycans. Some of the enzymes involved in the processing of glycans include N-acetylglucosaminyltransferase-I and -II (GnT1 and GnT2), galactosyltransferase, sialyltransferase, and fucosyltransferase. Addition of a non-reducing terminal GlcNAc to a precursor by GnT1 or GnT2 allows for the formation of complex and hybrid glycans.

#### *The Role of Fucosylation in Drosophila Neural Development*

Fucose addition to glycans frequently generates structures that mediate recognition events. Fucosylation of N-linked glycans or O-linked glycoproteins modulates specific cellular interactions and signaling. O-linked fucosylation of the Notch protein, catalyzed by O-fucosyltransferase 1 (OFUT1), alters its ability to signal downstream effectors. Fucose is commonly found in  $\alpha 6$  linkage to the reducing terminal N-acetylglucosamine (GlcNAc) residue of N-linked glycans. Fucose can also be added in an  $\alpha 1-3$  linkage to the same core GlcNAc, producing difucosylated glycans known as HRP-epitopes. One fucosyltransferase, FucTA, has been suggested to be responsible for the  $\alpha 3$  fucosylation that generates HRP-epitopes (Aoki et al.). HRP-epitopes are highly concentrated in the neural tissue of *Drosophila* embryos, especially in differentiating neurons. Thus, the presence of HRP-epitopes on the surface of developing

neurons serves as a signal for neural development. As neurons develop, Notch signaling attenuates, and HRP-epitope expression increases (Figure 3). The reciprocity between decreased Notch signaling and increased HRP-epitope expression suggests a shift in fucosylation resources (e.g. GDP-Fuc) and a regulatory mechanism for restricting Notch signaling. A dynamic equilibrium exists between the regulation of Notch signaling and the induction of fucosylation in neural development (Sharlow et al.) (Figure 4).

#### *Characterization of N-glycans in MS16-2 and *sff* Neural Tissues*

Studies on mutations in this essential fucosylation pathway could aid in understanding more about the pathway itself. In recent years, several members of Michael Tiemeyer's laboratory have carried out a mutagenesis screen to look for HRP-epitope glycosylation mutant lines in *Drosophila melanogaster*. The ethyl methane sulfonate (EMS) mutagenesis screen produced two mutants in the HRP biosynthetic pathway: the sugar-free frosting (*sff*) line and the MS16-2 line. The *sff* line is a mutation in the 3<sup>rd</sup> chromosome and the MS16-2 line is a mutation in the 2<sup>nd</sup> chromosome. Anti-HRP staining of *sff*, MS16-2, and *w*<sup>1118</sup> embryos (Figure 5) revealed that there is reduced HRP-epitope staining in *sff* and MS16-2 compared to *w*<sup>1118</sup>, a control phenotype.

Obtaining the total N-glycan profile of the embryos and stage-specific neural tissue from these two mutation lines would reveal the distribution of the different types of N-glycan species in the mutants' neural tissue. Most importantly, the distribution of HRP-epitopes in each profile could be indicative of the nature of the mutation. The detected amount of HRP-epitope in the neural tissue of *sff* and MS16-2 could also be used to confirm the anti-HRP staining. To further study the nature of the two fucosylation mutants, geotaxis behavioral testing was performed to

characterize the behavior of *sff* and MS16-2 adult flies. Defects in the movement of the two mutant lines could give insight into what aspect of neural function is impacted by the mutation. A study of the nature of these mutations would shed some light on a relatively unknown pathway that could be beneficial in the application of neural development in humans, with possibilities in dealing with neurodegenerative diseases.

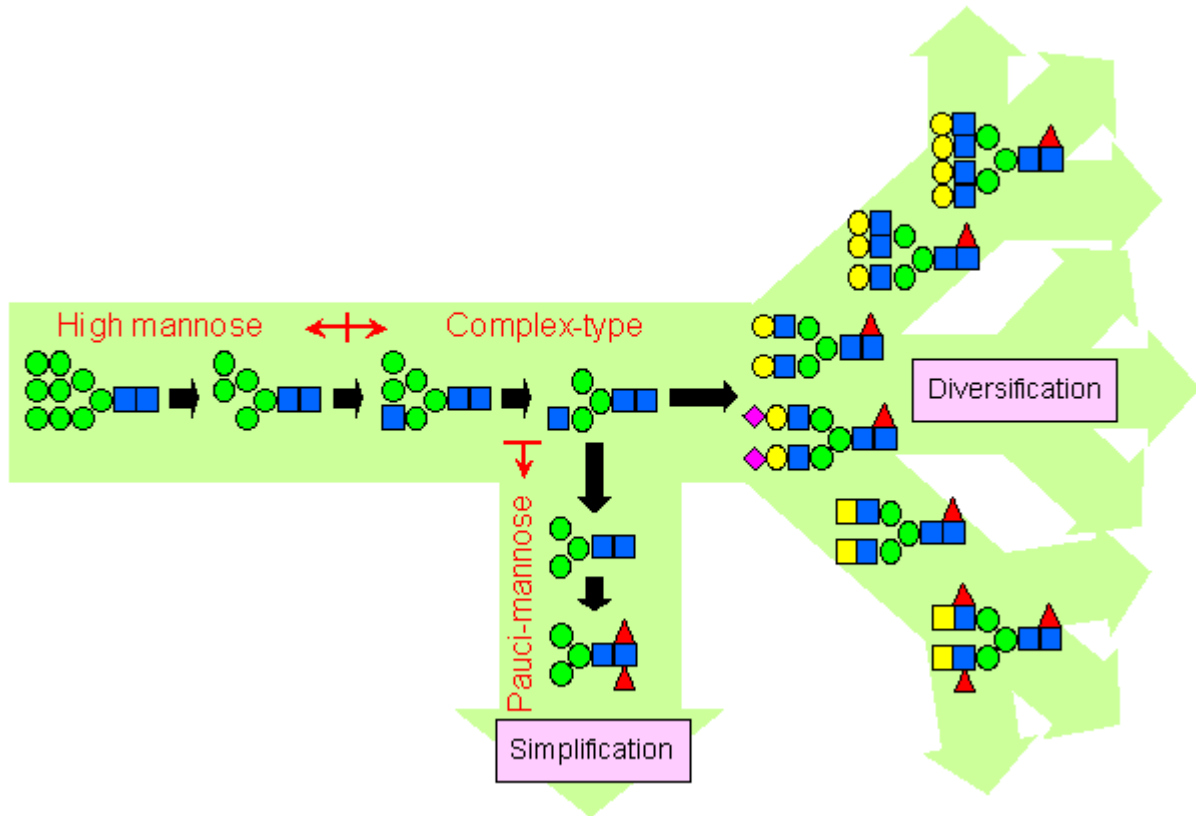


Figure 1. **Pathway of N-glycan processing and modification.** The pauci-mannose pathway could be used to divert resources away from the complex pathway. Legend: blue square = GlcNAc, green circle = mannose, red triangle = fucose, yellow circle = galactose, yellow square = GalNAc, purple diamond = NeuAc

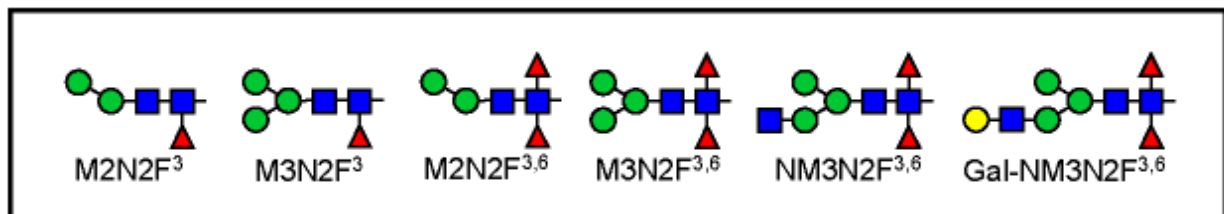


Figure 2. **Detected HRP-epitopes in *Drosophila* embryo.** HRP-epitopes are characterized by a fucose in  $\alpha 1-3$  linkage to the core GlcNAc.

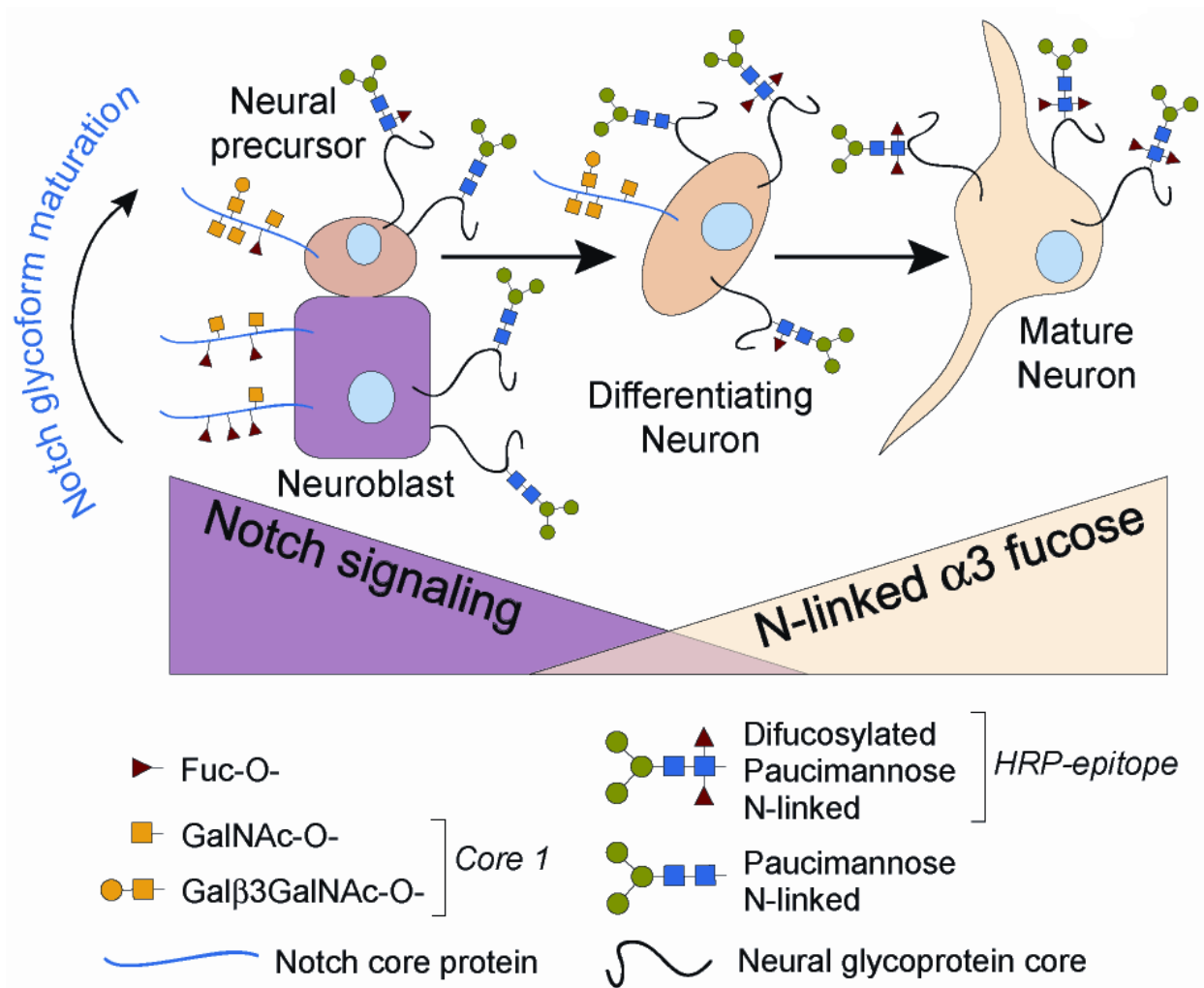


Figure 3. Differentiation of neurons is driven by attenuation of Notch signaling and increased production of HRP-epitope.

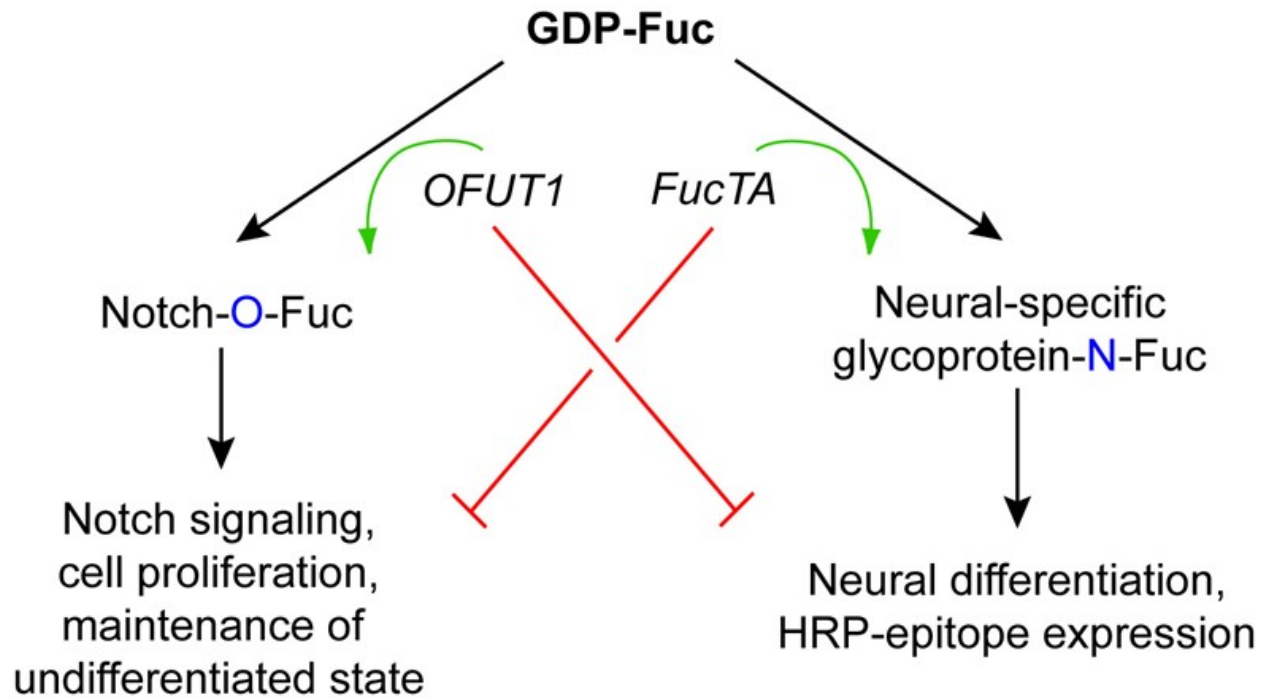


Figure 4. **Dynamic relationship between O-linked fucosylation of Notch and N-linked fucosylation in signaling neural differentiation.** The downstream effects of O-fucosylation of Notch by OFUT1 could regulate the N-fucosylation of glycans by FucTA. In turn, downstream effects of FucTA activity could regulate OFUT1 activity.

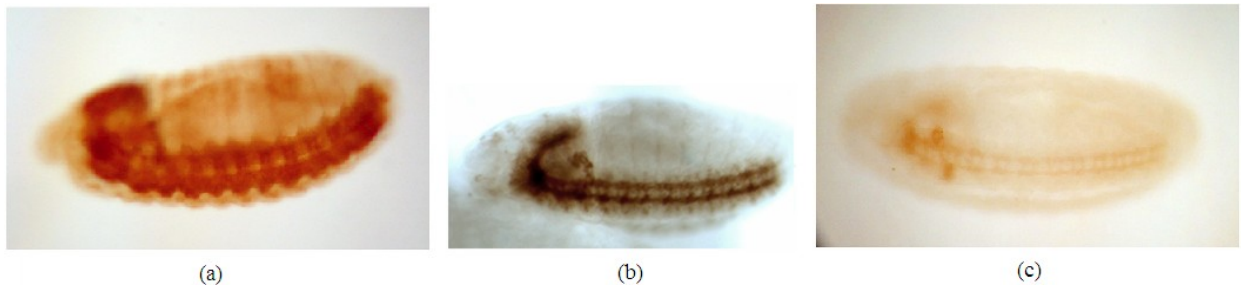


Figure 5. **Anti-HRP-epitope staining of  $w^{118}$ , MS16-2, and *sff* embryos.** Anti-HRP staining of (a)  $w^{118}$  embryos shows staining of the central nerve cord, peripheral nervous system, garland glands, and posterior hindgut. Staining of (b) MS16-2 embryos shows decreased staining in the central nerve cord and peripheral nervous system. Staining of (c) *sff* embryos show a more severe deficiency in staining.

## CHAPTER 2 MATERIALS AND METHODS

### *Drosophila Lines*

Two mutated *Drosophila* lines, *sff* and MS16-2, were generated from an ethyl methane sulfonate (EMS) mutagenesis screen performed by members of Michael Tiemeyer's laboratory. The EMS dosage used was enough to produce 2-3 hits per chromosome. The MS16-2 mutation has a line in a  $w^{1118}$  background, and the *sff* mutation has a line in a  $w^{1118}$  background and another line in an OreR background.

### *Embryo, Larval Brains, and Adult Heads Collection*

MS16-2 and  $w^{1118}$  flies were placed on apple juice collection plates with a small scoop of yeast and water mixture. The collection plates were incubated overnight for 16-18 hours at 25°C. After incubation, embryos were dechorionated by washing for 4 minutes in 50% bleach. The dechorionated embryos were washed with de-ionized water and filtered on Nytex filter mesh. The embryos were transferred to heptane in 1.5 mL Eppendorf tubes, and stored at -80°C.

The brains of third-instar  $w^{1118}$  and  $w^-$ ; *sff* larvae were dissected in 1x PBS using micro forceps. The brains were collected and stored in heptane in 1.5-mL Eppendorf tubes at -80°C. The total number of brains collected amounted to ~100 uL in wet volume for each phenotype, which is equivalent to ~500 larval brains for each phenotype.

The heads of four *Drosophila* phenotypes were collected:  $w^{1118}$ ,  $w^-$ ; *sff*, OreR, and  $w^+$ ; *sff*. Males from each phenotype were aged to 8 days at 18°C and subsequently decapitated with a razor blade. The heads were collected and stored dry in Eppendorf tubes at -80°C. The total number of heads collected amounted to ~200 uL dry volume for each phenotype.

#### *Glycan Preparation and Nanospray Ionization-Linear Ion Trap Mass Spectrometry*

Collected embryos, larval brains, and adult heads were de-lipidated by the method described by Kazuhiro Aoki (Aoki et al.) (Figure 6). The tissues were disrupted on ice by Dounce homogenization in ice-cold water. Lipids were extracted by adjusting the final solvent mixture to give a ratio of chloroform/methanol/water equal to 4:8:3. The extract was nutated for ~18 hours at room temperature, and then centrifuged in order to collect the lipid supernatant. The lipid components were re-extracted once more by adding 4 mL of prepared 4:8:3 chloroform/methanol/water mixture to the homogenized tissues and nutating for ~2 hours. The de-lipidated tissues were washed twice with 2 mL of acetone each time. The final pellet of protein was dried under a stream of N<sub>2</sub> gas. The resulting powder was stored at -20°C. About 32 mg of  $w^{1118}$  fly embryo powder was obtained from ~450 uL wet weight of embryos and approximately 15 mg of MS16-2 embryo powder was obtained from ~200 uL wet weight. Approximately 1-2 mg of powder was obtained from each of the brain and head phenotypes.

The collected lipid extracts were dried under a N<sub>2</sub> stream and the total lipid amount of  $w^{1118}$  and MS16-2 samples were determined by gas chromatography-mass spectrometry (GC/MS). The ratio of total lipid amount in  $w^{1118}$  and MS16-2 was 2:1, respectively. The total protein content of  $w^{1118}$  and MS16-2 samples were determined by BCA assay. The ratio of total protein amount in  $w^{1118}$  and MS16-2 was 2:1, respectively. These ratios were used to normalize the relative peak intensities in the total glycan profiles obtained. BCA assays were also

performed on the larval brain and adult head samples and the obtained ratios were used to normalize the total glycan profiles.

The processed protein powder was subjected to trypsin/chymotrypsin and PNGase F/A digestion in order to release the N-glycans from the protein (Figure 7). The protein powders (~3 mg of embryo powder and all of the brain and head powder) were placed in 1.5 mL plastic Eppendorf tubes and resuspended in 200 uL of trypsin buffer (0.1 M Tris-HCl, pH 8.2, containing 1 mM CaCl<sub>2</sub>). The mixture was boiled for 5 minutes at 100°C and cooled to room temperature. After cooling, 25 uL of freshly prepared trypsin and chymotrypsin (2 mg/mL in trypsin buffer) were added to the mixture and incubated at 37 C for 16-18 hours. After incubation, the mixture is boiled for 5 minutes. The supernatant was removed by centrifugation at 4 C, and dried down by vacuum centrifugation.

The dried down peptide mixture was resuspended in ~500 uL of 5% acetic acid (v/v) and loaded onto a Sep-Pak C18 column that was equilibrated with 3 mL of acetonitrile and 5 mL of 5% acetic acid. The column was washed with ~6 mL of 5% acetic acid. Glycopeptides were eluted first with 2 mL of 20% isopropanol in 5% acetic acid, and then with 2 mL of 40% isopropanol in 5% acetic acid. The two eluates were combined and dried by vacuum centrifugation.

For PNGase F digestion, the dried glycopeptides were resuspended in 25 uL of H<sub>2</sub>O and 20 uL of PNGase F buffer (0.1 M sodium phosphate, pH 7.5) and 5 uL of PNGase F (suspended as 7.5 U/mL). For PNGase A digestion, the dried glycopeptides were resuspended in 47 uL of PNGase A buffer (0.5 M citrate-phosphate, pH 5.0) and 3 uL of PNGase A (suspended as 5 mU/50 uL). The PNGase mixture is incubated for 16-18 hours at 37°C. After incubation, the mixture is boiled for 5 minutes and dried by vacuum centrifugation.

The released glycans are separated from the protein and enzyme in the dried mixture by use of a Sep-Pak C18 column. The dried mixture is resuspended in ~500 uL of 5% acetic acid and loaded onto an equilibrated column. The released glycans are eluted with ~4 mL of 5% acetic acid and dried on a lyophilizer.

In order to prepare the released glycans for analysis by mass spectrometry, small portions of the glycans were permethylated with [ $^{12}\text{C}$ ] methyl iodide. The base reagent for permethylation was prepared from 100 uL of 50% NaOH, 200 uL of anhydrous methanol, and 2 mL of anhydrous dimethyl sulfoxide (DMSO). The glycans were resuspended in 200 uL of anhydrous DMSO and dissolved mixture in  $\text{N}_2$  gas. 250 uL of base and 100 uL of [ $^{12}\text{C}$ ] methyl iodide were added to the mixture, and dissolved the mixture in  $\text{N}_2$  gas. 2 mL of de-ionized water was added to the mixture. The excess [ $^{12}\text{C}$ ] methyl iodide was removed by purging the mixture with  $\text{N}_2$  gas. The permethylated glycans were extracted by adding 2 mL of dichloromethane (DCM). The aqueous layer was removed and additional washes with de-ionized water were performed. After 5 washes, the organic layer is dried down under  $\text{N}_2$  gas. To compare relative glycan abundances in MS16-2 and w<sup>1118</sup> embryo samples, released glycans were permethylated with [ $^{13}\text{C}$ ] methyl iodide or [ $^{12}\text{C}$ ] methyl iodide, respectively, and combined before analysis by NSI-MS. The ratio of the peaks intensities for differently labeled glycans in the same spectra shows the relative abundance of each glycan in the two glycan preparations.

Permethylated glycans were analyzed by nanospray ionization-linear ion trap mass spectrometry (NSI-MS). The glycans were dissolved in 1 mM NaOH in 50% methanol and injected directly into a linear ion trap mass spectrometer (LTQ; Thermo Finnigan) with a nanoelectrospray source at a syringe flow rate of 0.40-0.60 uL/min. The capillary temperature was set at 210 C, and analysis was performed in positive ion mode. For fragmentation analysis

by collision-induced dissociation (CID) in tandem mass spectrometry (MS/MS) mode, 28% collision energy was used.

The XCalibur software package (version 2.0) was used in the analysis of the MS data. The total ion mapping (TIM) function of the software package was utilized to detect and quantify the prevalence of individual glycans in the total glycan profile. Using TIM, automated MS spectra were obtained in 2.8 mass units windows. An average of five scans, each lasting 150 ms, was applied to each collection window. A  $m/z$  range of 200 to 2000 was scanned in each window.

Most permethylated glycans were identified as singly and double charged species in NSI-MS. The TIM peaks from all charge states of all species with  $m/z < 2000$  were used together in quantifying the total glycan profile. The prevalence of a glycan was calculated as the percentage of the total profile where the total profile is the sum of the peak intensities of all identified glycans. The MS/MS spectra for all TIM peaks were examined for daughter ions indicative of a glycan species.

#### *Geotaxis Testing*

Four-day old male  $w^{1118}$ , MS16-2, and *sff* flies were individually placed into a clear plastic vial (2 cm diameter, 7 cm length) with no food. The flies were starved for 4 hours at 18°C. After starving, the flies were tapped down to the bottom of the vial and the movement of the fly up the wall of the vial was observed for 120 seconds. The time taken for the fly to climb to the top of the vial was recorded.

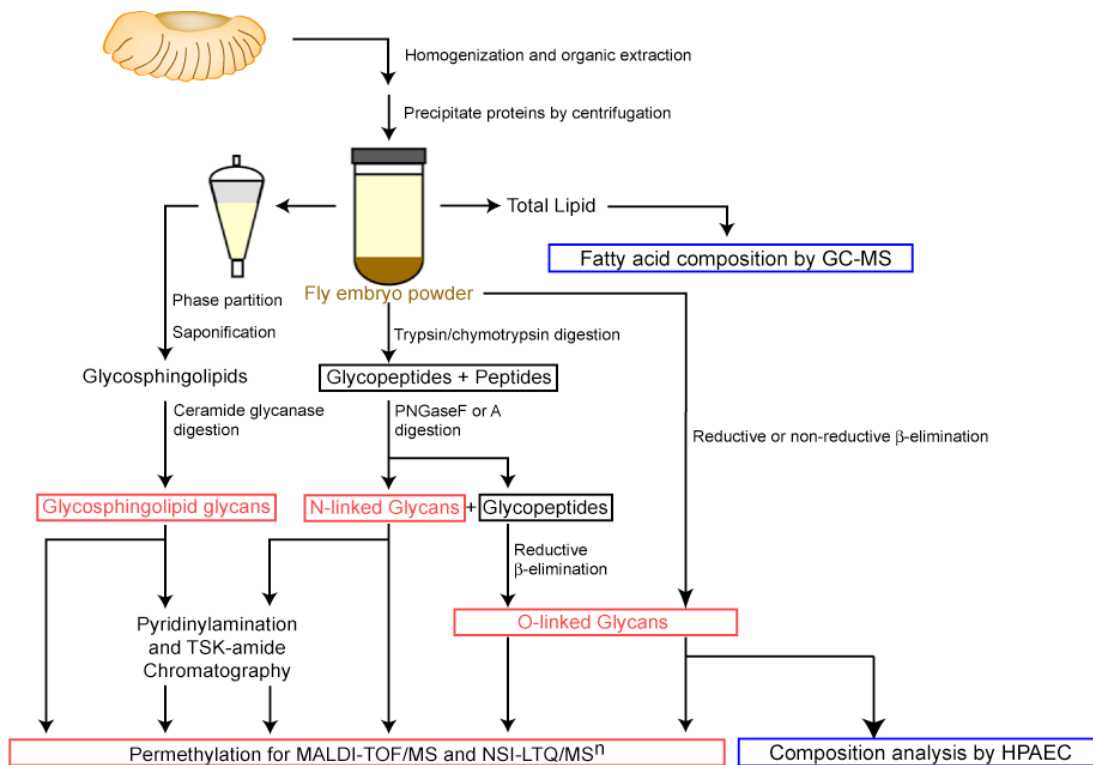


Figure 6. **Tissue preparation and processing for glycan analysis.** Embryos are initially de-lipidated and formed into a protein powder. The protein powder can then be used to analyze for N- and O-linked glycans.

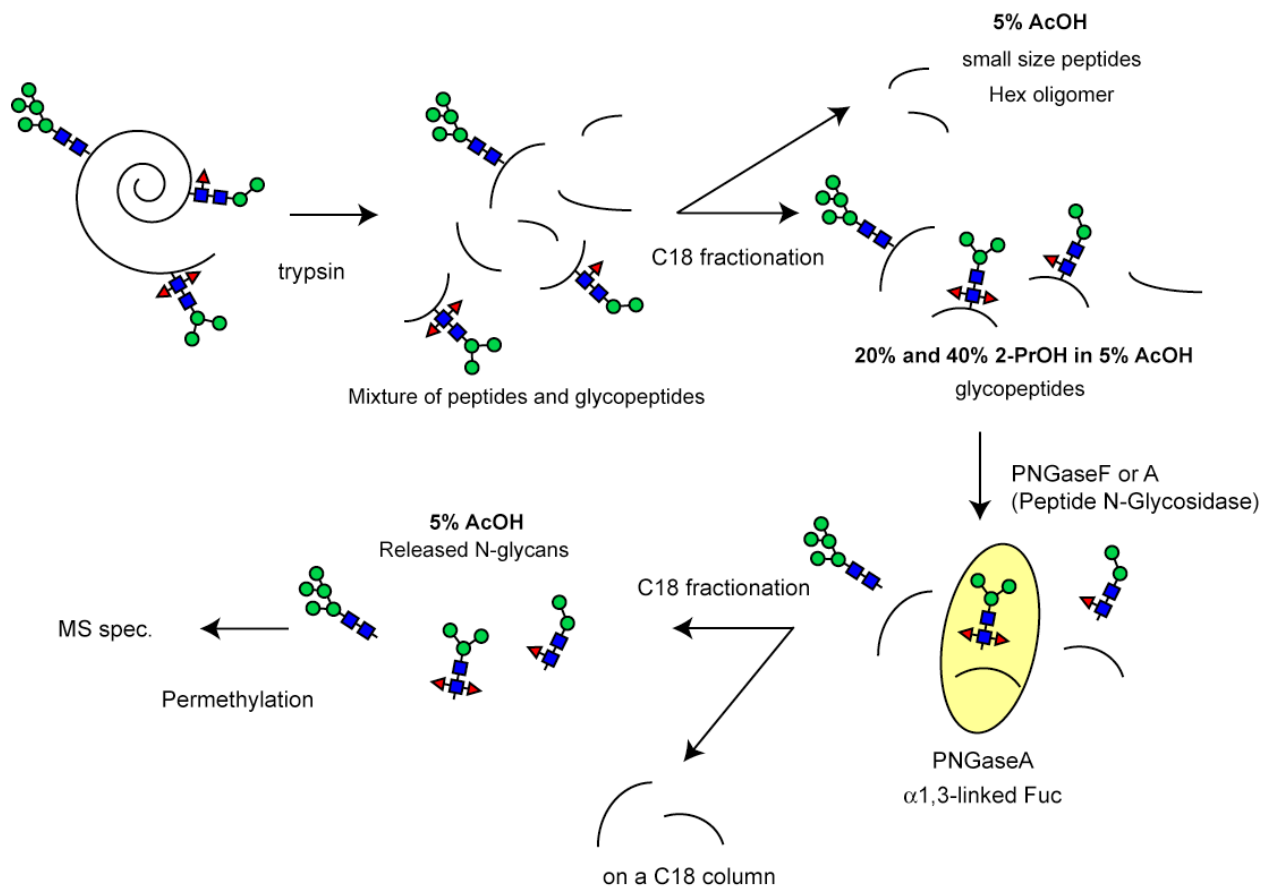


Figure 7. **Release of N-glycans from protein powder.** Protein powder is first digested with trypsin/chymotrypsin and purified for glycopeptides through C18 fractionation. Glycopeptides are then digested with PNGase F or A to release glycans for analysis.

### CHAPTER 3 CHARACTERIZATION OF N-GLYCANS IN MS16-2 AND W<sup>1118</sup> EMBRYOS

Comparing the N-glycan profile of MS16-2 embryos to a control, w<sup>1118</sup>, could be useful in determining any differences in N-glycan expression. The differences in N-glycan expression could provide insight to any alterations in the biosynthetic pathway of N-glycans in MS16-2 embryos compared to wild-type embryos. More importantly, examining the alteration in HRP-epitope expression in MS16-2 embryos could be a good step in figuring the cellular mechanisms involved in regulating fucosylation and neural differentiation.

#### *Total N-Linked Glycan Profile of w<sup>1118</sup> and MS16-2*

The total profiles for N-linked glycans released from w<sup>1118</sup> and MS16-2 embryo powder by PNGase A exhibit a dominance of high mannose (M5N2, M6N2, M7N2, M8N2, and M9N2) and monofucosylated (M2N2F and M3N2F) glycans (Figure 8). This dominance in high mannose and monofucosylated pauci-mannose structures is characteristic of wild-type embryos (Aoki et al.). The dominance of these structural types obstructs the identification of minor components from the profile. With closer inspection of the profile, however, the minor glycan components of both profiles is seen to include complex structures with terminal GlcNAc on the trimannosyl core (NM4N2, NM3N2, N3M3N2, and N2M5N2) and monofucosylated glycans with terminal GlcNAc (N2M4N2F, N2M3N2F, N2M2N2F, and NM3N2F). Overall, the total profiles of w<sup>1118</sup> and MS16-2 look similar, and the prevalence of most identified glycan are also similar in both (Figure 9). One significant difference between the two profiles is the increased

expression of monofucosylated pauci-mannose structures (M2N2F, M3N2F, etc.) and glycans bearing one nonreducing terminal GlcNAc (NM2N2, NM3N2, etc.) in MS16-2 embryos relative to w<sup>1118</sup> embryos. This shift in the N-glycan biosynthetic pathway could be indicative of the activity of the MS16-2 mutation.

#### *Release and Detection of Difucosylated Glycans*

Glycan release by PNGase F is restricted for N-linked oligosaccharides that have fucose-linked  $\alpha$ 1-3 to the internal GlcNAc of the chitobiose core, while PNAase A is not restricted by core fucosylation. Digestion with PNGase A allows for the release and detection of HRP epitopes. The detection of difucosylated glycans (M2N2F2, M3N2F2, and NM3N2F2) from the total PNGase A profile is difficult due to the low peak intensities. However, analysis of fragmentation patterns of HRP epitopes reveals a decrease in these glycans in MS16-2. The fragmentation pattern of M3N2F2 ( $m/z = 1520$ ) for w<sup>1118</sup> and MS16-2 embryos reveal a six-fold decrease in the peak intensities in MS16-2 relative to w<sup>1118</sup> (Figure 10). The detection of decreased HRP-epitope expression in the total N-glycan profile of MS16-2 embryos confirm the anti-HRP staining of MS16-2 embryos, which also reveal a significant decrease in HRP-epitope expression.

#### *Differential Isotopic Labeling of Glycans*

Using [<sup>13</sup>C] methyl iodide and [<sup>12</sup>C] methyl iodide to differentially label w<sup>1118</sup> and MS16-2 samples allows for comparing the peak intensities of glycans between the two samples. Figure 11 shows a profile that contains both <sup>13</sup>C and <sup>12</sup>C labeled glycans; w<sup>1118</sup> glycans were labeled with <sup>12</sup>C and MS16-2 glycans were labeled with <sup>13</sup>C. The profile shows that the abundance of glycans in the MS16-2 sample is significantly higher than in the w<sup>1118</sup> sample. Since this is only the initial

differential labeling performed, it is not conclusive that MS16-2 truly expresses a larger quantity of N-glycans. At least one more differential preparation is needed in order to confirm the quantity of glycans.

One interesting finding from the differential preparation is that the peak intensity for M3N2F2, an HRP epitope, is greater in the w<sup>1118</sup> sample preparation despite the lesser abundance of other glycan species compared to the MS16-2 preparation. The peak intensity for M3N2F2 from w<sup>1118</sup> is almost twice as much as the peak from MS16-2 (Figure 12).

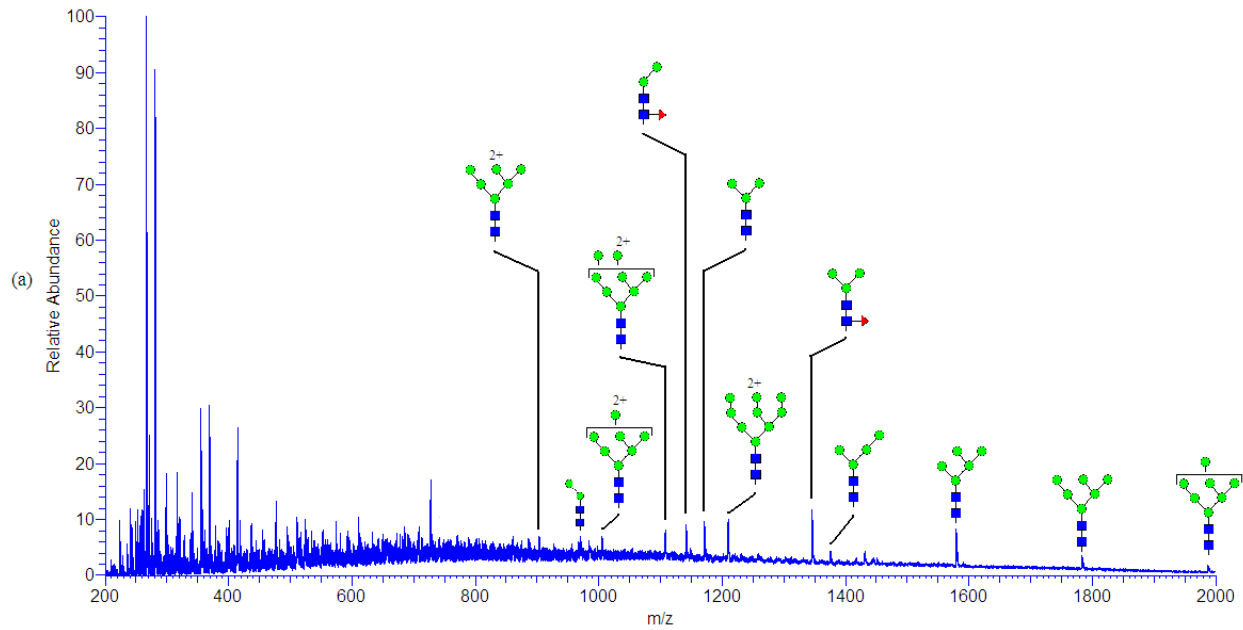
#### *Possible Alterations in N-Glycan Biosynthesis Attributed to MS16-2 Mutation*

The total N-glycan profiles obtained from PNGase F and A digestion of MS16-2 and w<sup>1118</sup> embryo protein powder, and subsequent differential isotopic labeling support the observation that there is a decrease in HRP-epitope expression in MS16-2 embryos, as indicated by the anti-HRP staining of MS16-2 embryos. These N-glycan profiles, along with the profiles obtained from the differential isotopic labeling preparation, confirm the role of the MS16-2 mutation in altering HRP-epitope expression. Interestingly, coincidental with the decrease in difucosylated N-glycans is the increase in monofucosylated structures in MS16-2. This inverse relationship between the quantities of monofucosylated and difucosylated N-glycans in MS16-2 could suggest a defect in the ability of the MS16-2 embryo to add a fucose in a  $\alpha$ 1-3 linkage to the chitobiose core of the precursor oligosaccharide. MS16-2 could possibly be a defect in the expression of a  $\alpha$ 3 fucosyltransferase; diminished genetic expression of the fucosyltransferase or a defective enzymatic product is possible. The inability of MS16-2 to synthesize or transport GDP-fucose for fucosylation is unlikely, as the amount of monofucosylated structures in MS16-2 embryos is increased. Another possibility is that the mutation in MS16-2 is a defective signaling component that regulates the synthesis of HRP-epitopes.

Another significant result is the increase in expression of pauci-mannose structures, which could be suggestive of a shift in the biosynthetic pathway of N-glycans away from complex glycans. The shift in N-glycan biosynthesis could be related to the decrease in HRP-epitope expression; the increase in pauci-mannose structures could divert the resources that would normally be used for HRP-epitope biosynthesis. Further N-glycan analysis to detect the complete abundance of complex glycans is necessary in order to support this notion.

N-linked glycan analysis has only been performed on MS16-2 embryos, which limits the amount insight on how the mutation has an effect on later neurological development, such as in the larval and adult stage. Analysis of N-linked glycans at these later stages could track the progression of the effects of the MS16-2 mutation. Most importantly, mapping the MS16-2 mutation would be infinitely useful in determining what the mutation actually is.

KA-FP-W1118-PNGA\_080407124546 #1-68 RT: 0.00-1.00 AV: 68 NL: 6.51E4  
T: ITMS + p NSI Full ms [200.00-2000.00]



KA-FP-MS16-PNGA\_080407120904 #1-69 RT: 0.00-1.01 AV: 69 NL: 7.41E4  
T: ITMS + p NSI Full ms [200.00-2000.00]

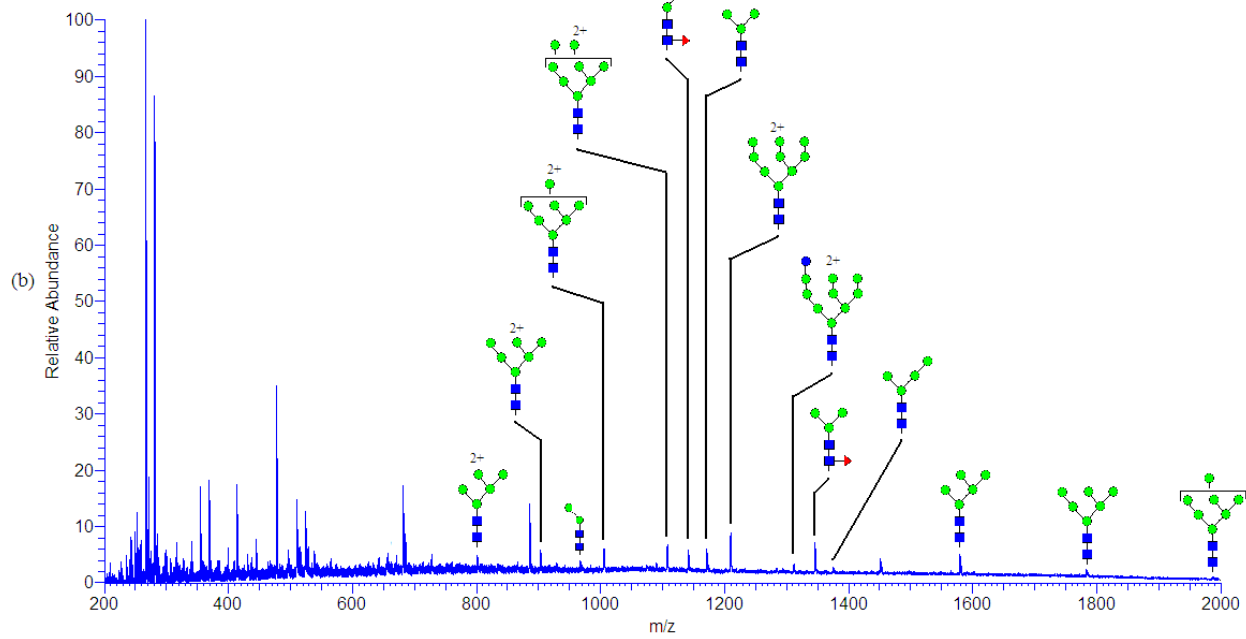


Figure 8. N-linked glycan profile released by PNGase A. Total profile for (a)  $w^{1118}$  and (b) MS16-2 embryos.

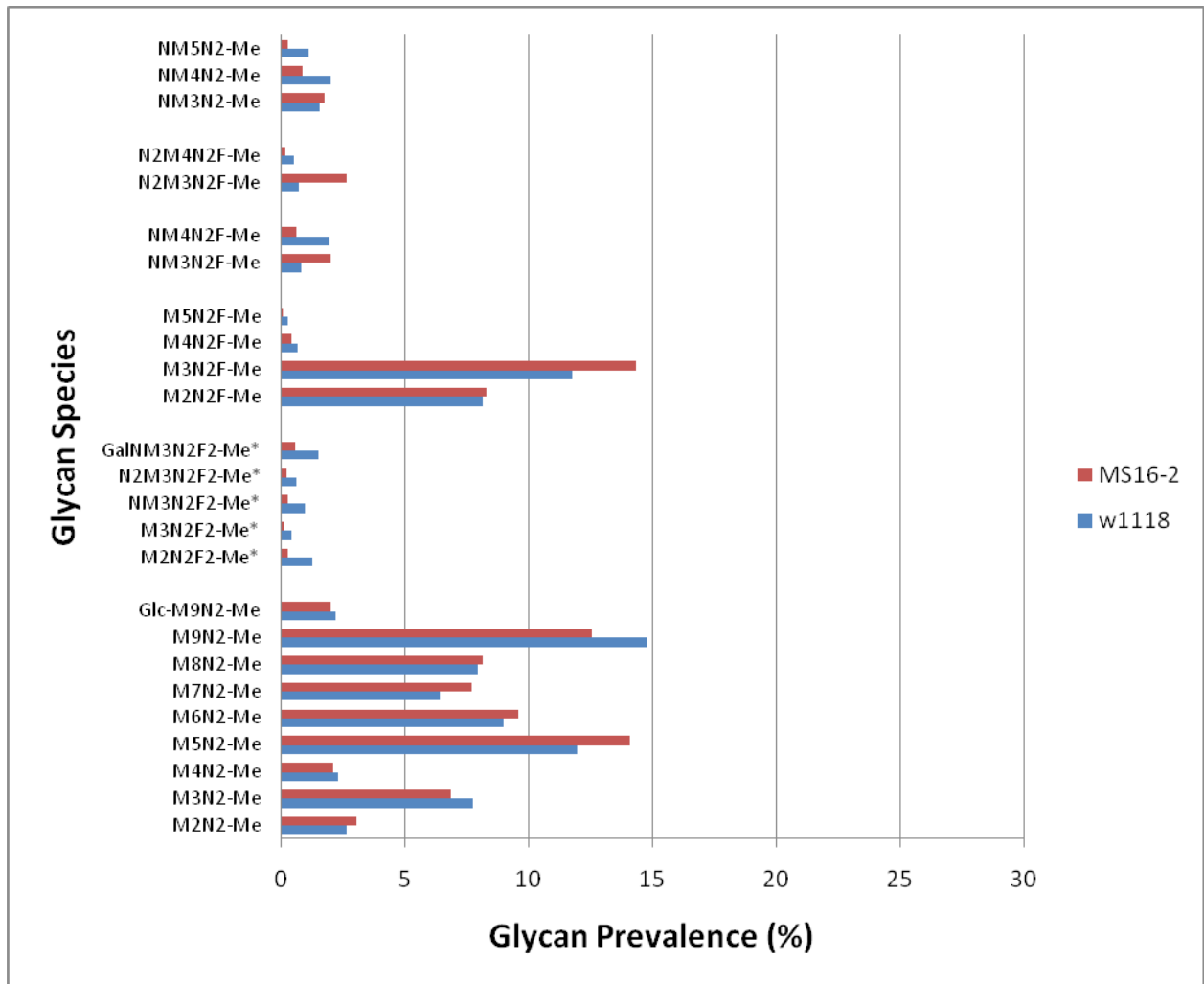


Figure 9. N-glycan prevalence of w<sup>1118</sup> and MS16-2 embryos. The N-glycan prevalence of w<sup>1118</sup> and MS16-2 are similar. \* = HRP-epitopes.

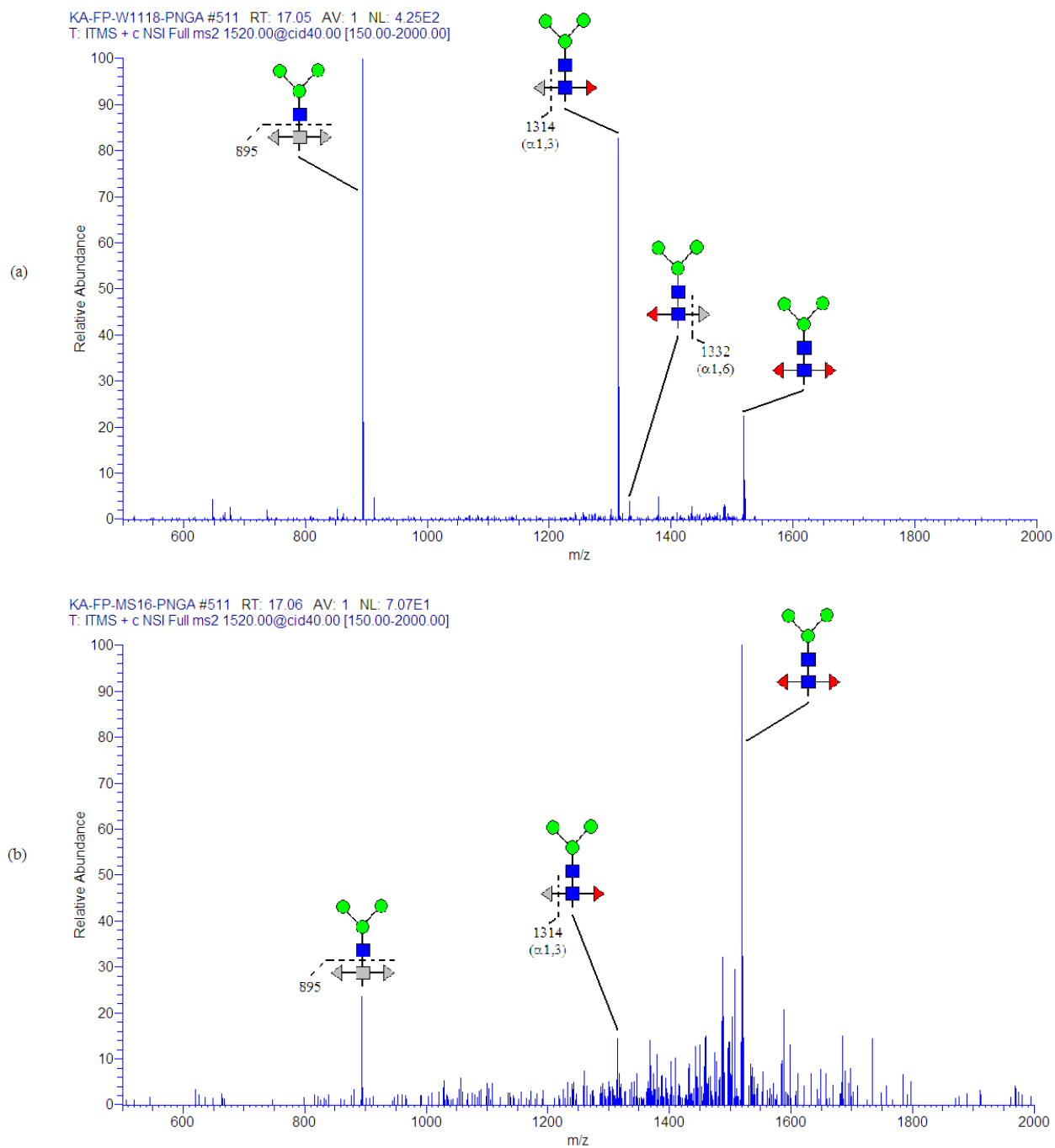


Figure 10. **Fragmentation pattern of M3N2F2 (mass = 1520).** Patterns from (a)  $w^{1118}$  and (b) MS16-2 show a reduction in loss-of-fucose fragmentations.

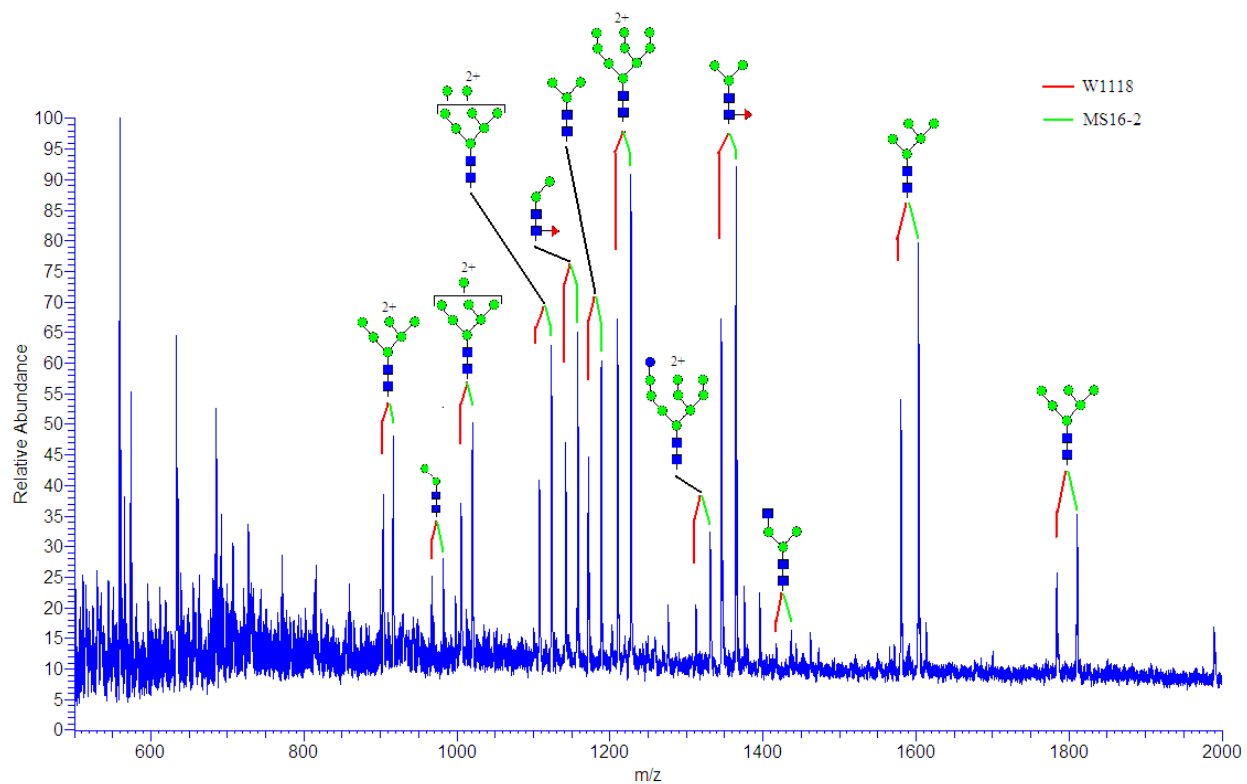


Figure 11. **Differential N-glycans profile of w<sup>1118</sup> and MS16-2.** The profile shows a larger abundance of N-glycans in MS16-2.

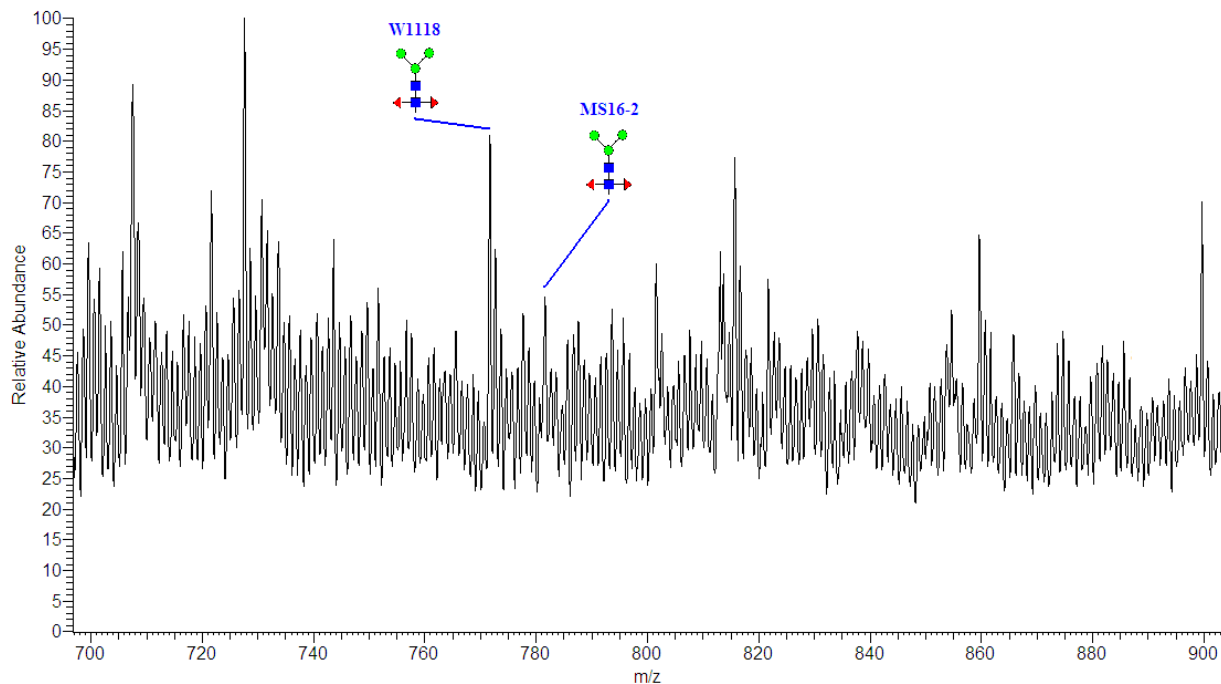


Figure 12. **Differentially labeled M3N2F2 peaks for  $w^{1118}$  and MS16-2.** The peak for M3N2F2 from  $w^{1118}$  is almost twice as much as the peak for MS16-2.

## CHAPTER 4 N-GLYCAN EXPRESSION AT *sff* LARVAL AND ADULT STAGES

### *N-glycan Profile of Larval *sff* and *w*<sup>1118</sup> Brains*

Total N-glycan profiles were generated from the released glycans of protein powder processed from dissected *w*<sup>-</sup>; *sff* and *w*<sup>1118</sup> larval brains (Figure 13). In general, the profiles of both samples are dominated by high mannose and monofucosylated pauci-mannose glycans. Minor glycan components include complex structures (e.g. GalNM3N2F2) and products of GnT1 and GnT2 (NM3N2F, NM2N2, NM3N2, etc.). Also, the glycan prevalence in both profiles are fairly similar, and most glycan species are expressed in identical levels (Figure 14). The most important difference between the two samples, however, is that HRP-epitope expression is greatly decreased in *w*<sup>-</sup>; *sff* larval brains. Another notable difference in the glycan prevalence is the increase of monofucosylated pauci-mannose glycans (M3N2F and M2N2F) in *w*<sup>-</sup>; *sff* larval brains. The amount of N-acetylglucosaminyltransferase products (NM3N2, NM2N2, etc.) and high mannose structures are decreased in *w*<sup>-</sup>; *sff*.

### *N-glycan Profile of Adult *sff* and Wild-Type Heads*

Two pairs of samples were analyzed for N-glycans: *w*<sup>1118</sup> and *w*<sup>-</sup>; *sff* (48w) adult heads, and OreR and *w*<sup>+</sup>; *sff* (48r) adult heads. The total N-glycan profiles for OreR and *w*<sup>+</sup>; *sff* adult heads (Figure 15) are generally similar in that there is a dominance of monofucosylated pauci-mannoses and high mannose structures. The distribution of the prevalence of glycan types is fairly similar between OreR and *w*<sup>+</sup>; *sff* adult heads (Figure 16). The most important difference in

the two profiles is the decrease of HRP-epitopes in  $w^+$ ; *sff* adult heads. Another major difference is the increase in monofucosylated pauci-mannose glycans in  $w^+$ ; *sff* adult heads. Minor differences include a general decrease in high mannose structures and a slight increase in GnT products (glycans with a non-reducing terminal GlcNAc). One interesting observation is the large decrease in M5N2, the oligosaccharide that is initially synthesized in the N-glycan biosynthetic pathway, in  $w^+$ ; *sff* adult heads.

The total N-glycan profiles of  $w^{1118}$  and  $w^-$ ; *sff* adult heads (Figure 17) is not as clean as the profiles for OreR and  $w^+$ ; *sff* adult heads, but the profiles are clean enough to make observations on the relative glycan prevalence in  $w^{1118}$  and  $w^-$ ; *sff* adult heads (Figure 18). The distribution of N-glycan species in  $w^-$ ; *sff* heads are identical to  $w^{1118}$  heads; both profiles contain a dominance of high mannose and monofucosylated pauci-mannose glycans. Again, there is a decrease in HRP-epitopes in  $w^-$ ; *sff* heads compared to  $w^{1118}$  heads. Interestingly, there is a decrease in monofucosylated pauci-mannose structures in  $w^-$ ; *sff* relative to  $w^{1118}$ , and an increase in complex glycans and GnT products. Also, there is a general decrease in high mannose glycans in  $w^-$ ; *sff*, except for an unusual increase in M5N2.

The distribution of N-glycan species in  $w^-$ ; *sff* adult heads are similar to the distribution in  $w^+$ ; *sff* adult heads; both profiles exhibit a dominance of high mannose and monofucosylated pauci-mannose structures. The profiles of  $w^-$ ; *sff* and  $w^+$ ; *sff* adult heads both show a decrease in HRP-epitopes. Surprisingly, the level of monofucosylated pauci-mannose glycans is decreased in  $w^-$ ; *sff* adult heads in comparison to  $w^+$ ; *sff* adult heads. Another surprise is the increase of GnT products (NM5N2 and NM4N2) in  $w^-$ ; *sff* adult heads relative to  $w^+$ ; *sff* adult heads.

In comparison to  $w^-$ ; *sff* larval brains,  $w^-$ ; *sff* adult heads exhibit a general increase in total N-glycan expression, which is expected in the higher developed adult head. There is an increase in HRP-epitope expression in  $w^-$ ; *sff* adult heads compared to  $w^-$ ; *sff* larval brains. An exception to this observation is the decrease of monofucosylated pauci-mannose structures in the adult head.

### *Speculations on sff Mutation*

All of the N-glycan analysis of *sff* larval brains and adult heads support the role of the *sff* mutation in decreasing HRP-epitope expression in neural tissue. The continued decrease in HRP-epitope expression into the larval and adult stage of *sff* flies suggests that the mutation is in effect throughout the full developmental cycle of the *sff* line. The decrease of HRP-epitopes in the N-glycan analysis of *sff* also confirms the anti-HRP staining of *sff* embryos; it is quite obvious that the *sff* mutation has an important role in tissue-specific fucosylation.

In comparing the N-glycans of  $w^-$ ; *sff* and  $w^{1118}$  larval brains, there is a general decrease in high mannose structures and GnT products in  $w^-$ ; *sff* and GnT products. There also is a general increase in monofucosylated pauci-mannose structures in  $w^-$ ; *sff*. This shift in N-glycan distribution could indicate an increase in the pauci-mannose biosynthetic pathway, diverting resources away from the synthesis of complex structures. In addition, the coincidental decrease in HRP-epitopes and increase in monofucosylated structures could indicate a shift in utilization of GDP-fucose or a defect in  $\alpha 3$  fucosylation of the core GlcNAc. Another possibility is that the *sff* mutation is a defective regulatory component in fucosylation during the biosynthetic pathway. The divergence in the synthesis of monofucosylated and difucosylated glycans in *sff* could

suggest a regulatory equilibrium between the syntheses of these two species, which could be limited by the supply of GDP-fucose.

Comparing the N-glycan profiles of  $w^-; sff$  larval brains to  $w^-; sff$  adult heads could provide insight to how N-glycan synthesis changes as neural development progresses and the role of the *sff* mutation in different stages of development. The general increase in HRP-epitopes and GnT products in the adult head relative to the larval brain could be indicative of higher neural development in the adult head, which is expected. The increase in GnT products could also be indicative of an increase in the synthesis of complex glycans (e.g. GalNM3N2F2). Another difference between the two stages of development is the decrease of monofucosylated pauci-mannose structures in *sff* adult heads. Again, this shift away from the pauci-mannose pathway could lead to an increase in synthesis of complex glycans. The decrease in monofucosylated pauci-mannose structures could just be a consequence of development, but it could also suggest that the role of the *sff* mutation in N-glycan biosynthesis changes in the adult stage.

In addition to the decrease of HRP-epitope expression in  $w^-; sff$  adult heads in relation to  $w^{1118}$  adult heads, there is also a decrease in the expression of M5N2 in  $w^-; sff$  adult heads. The decrease in monofucosylated pauci-mannose structures observed in the shift from  $w^-; sff$  larval brains to  $w^-; sff$  adult heads is also observed between  $w^{1118}$  and  $w^-; sff$  adult heads. This observation is suggestive of role of the *sff* mutation in regulating this shift away from monofucosylated pauci-mannose synthesis. Another interesting observation between  $w^{1118}$  and  $w^-; sff$  adult heads is a striking decrease in the level of M5N2 in  $w^-; sff$  adult heads. The synthesis of the oligosaccharide M5N2 is the very first step in N-glycan biosynthesis. The transport of

M5N2 into the rough ER lumen is necessary for the synthesis and processing of all other glycan species. This decrease of M5N2 in *w<sup>-</sup>*; *sff* adult heads could suggest that there is a defect in transporting M5N2 into the rough ER lumen.

N-glycan analysis of the neural tissue of *sff* developmental stages is helpful in elucidating the nature of the *sff* mutation. However, the extent of glycan analysis in learning more about the mutation is limited. The best way of learning about the mutation is to map the *sff* mutation itself.

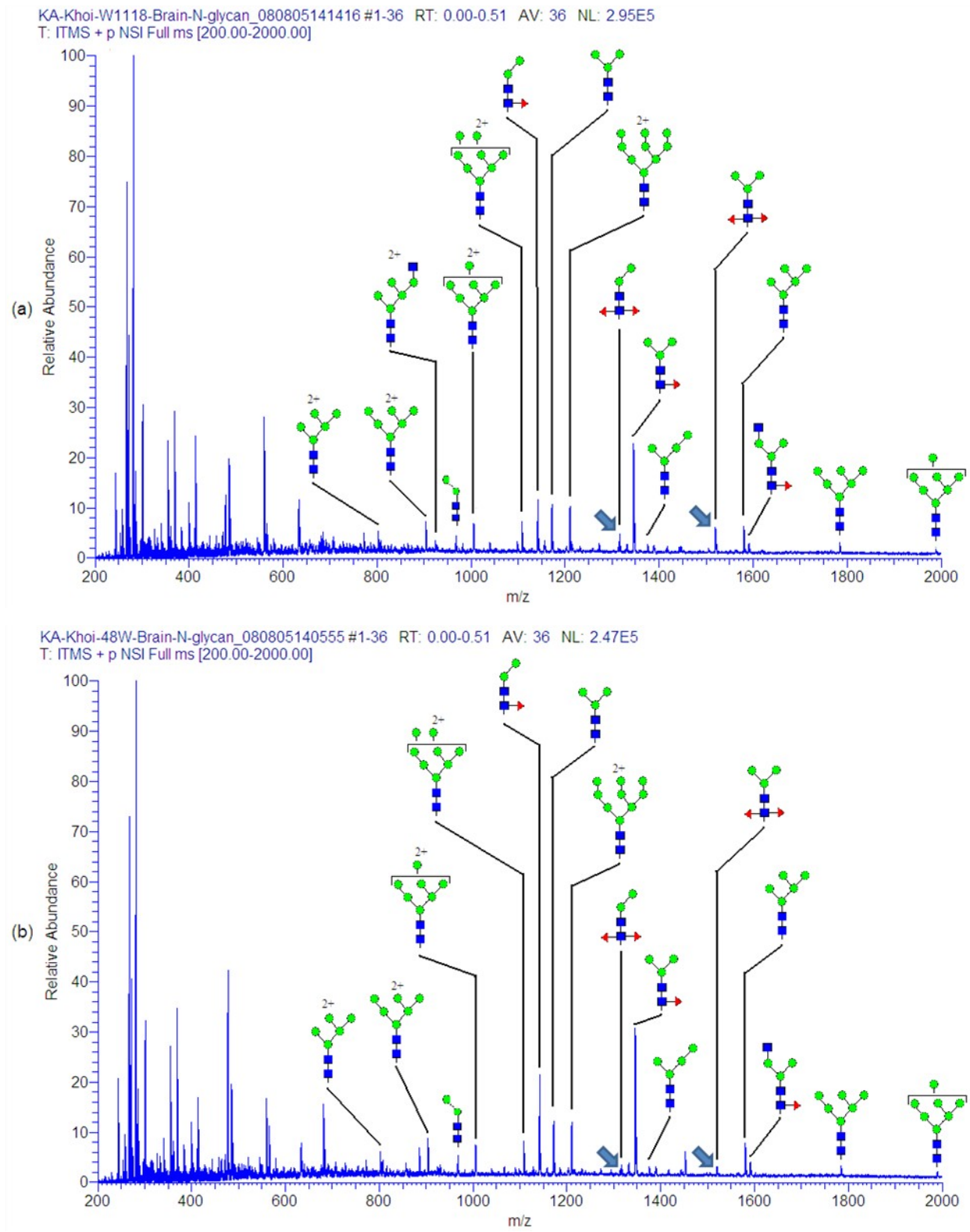


Figure 13. **N-linked glycan profile of  $w^{1118}$  and *sff* larval brains.** Total profile for (a)  $w^{1118}$  and (b) *sff* brains. Blue arrows indicate the apparent decrease in the HRP-epitopes.

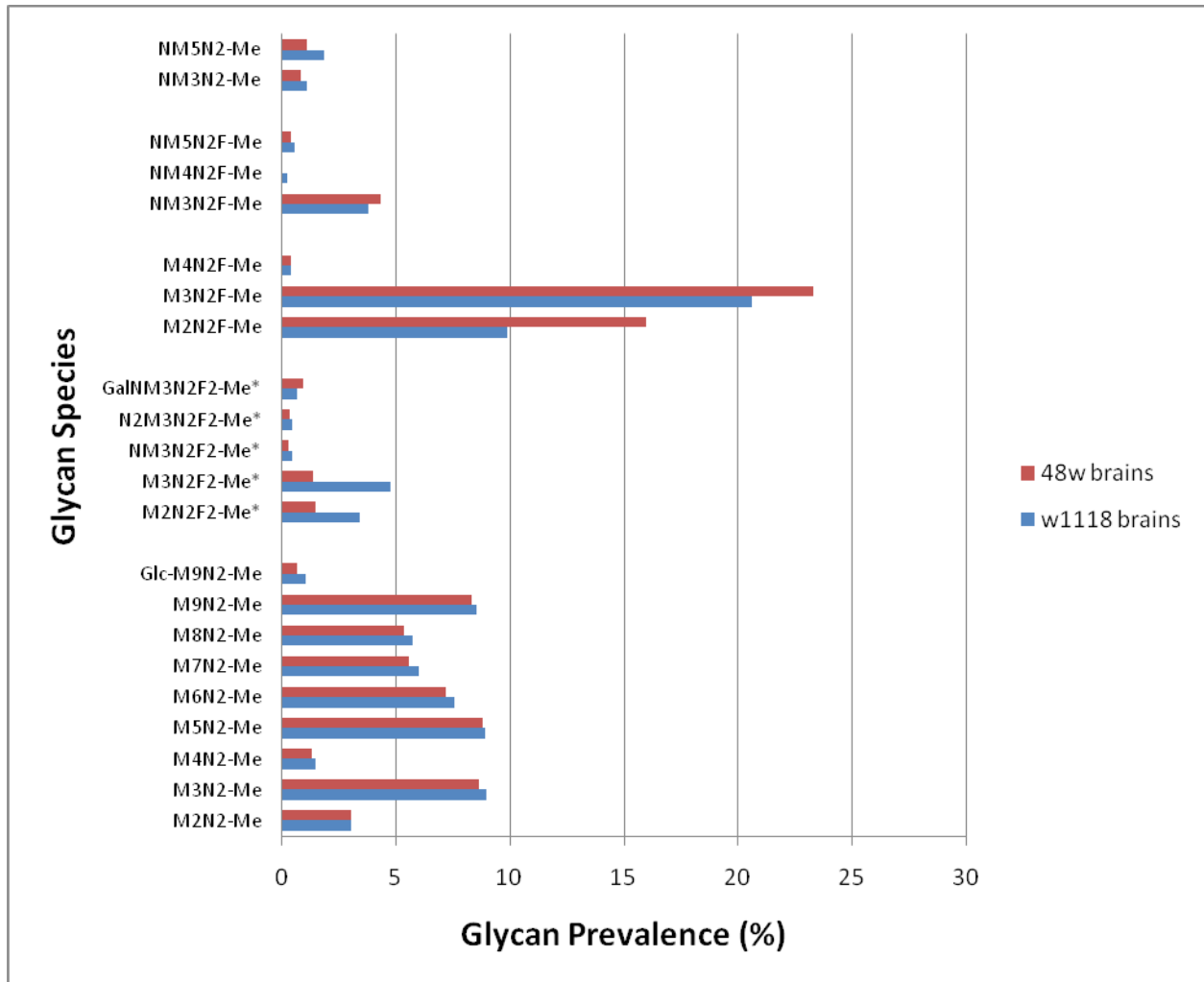
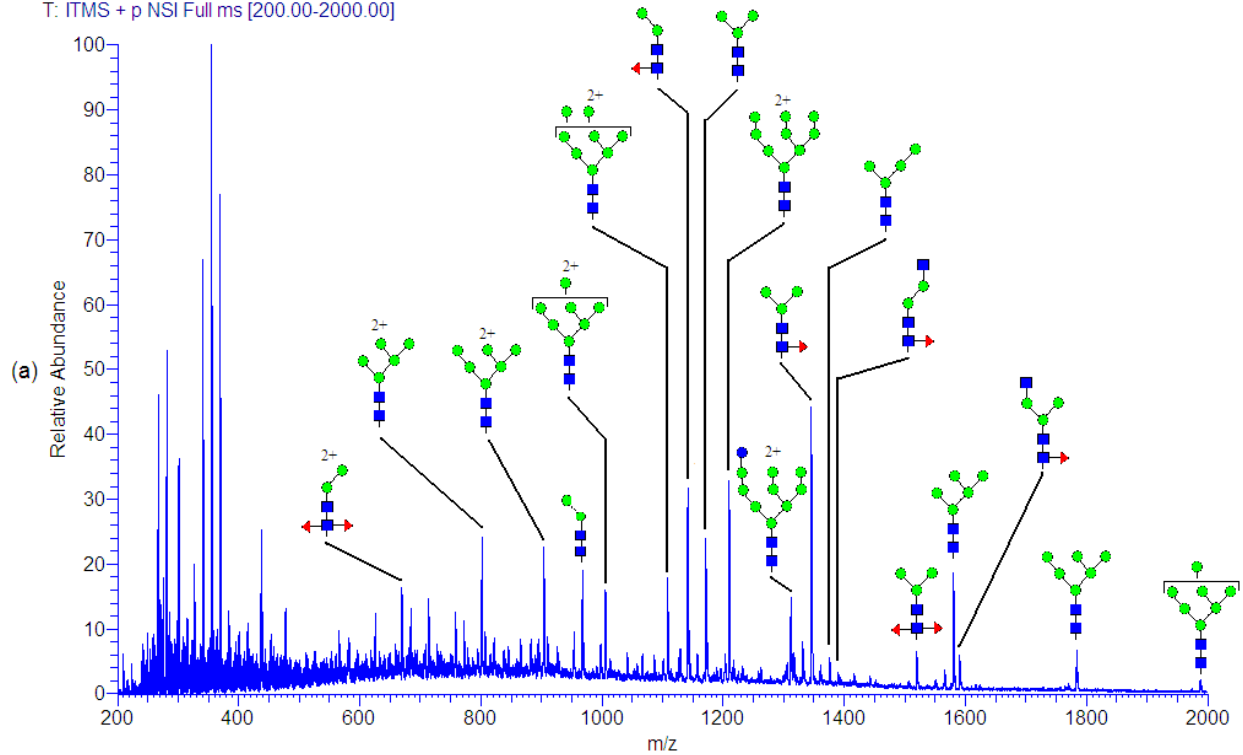


Figure 14. **N-glycan prevalence of  $w^{1118}$  and *sff* larval brains.** *sff* larval brains display a decrease in HRP-epitopes(\*) and an increase in monofucosylated structures.

KA-Sarah-OreR-head-PNGA\_080911102229 #1-34 RT: 0.00-0.50 AV: 34 NL: 4.37E4  
T: ITMS + p NSI Full ms [200.00-2000.00]



KA-Sarah-48r-head-PNGA\_080911112125 #1-38 RT: 0.00-0.51 AV: 38 NL: 5.02E4  
T: ITMS + p NSI Full ms [400.00-2000.00]

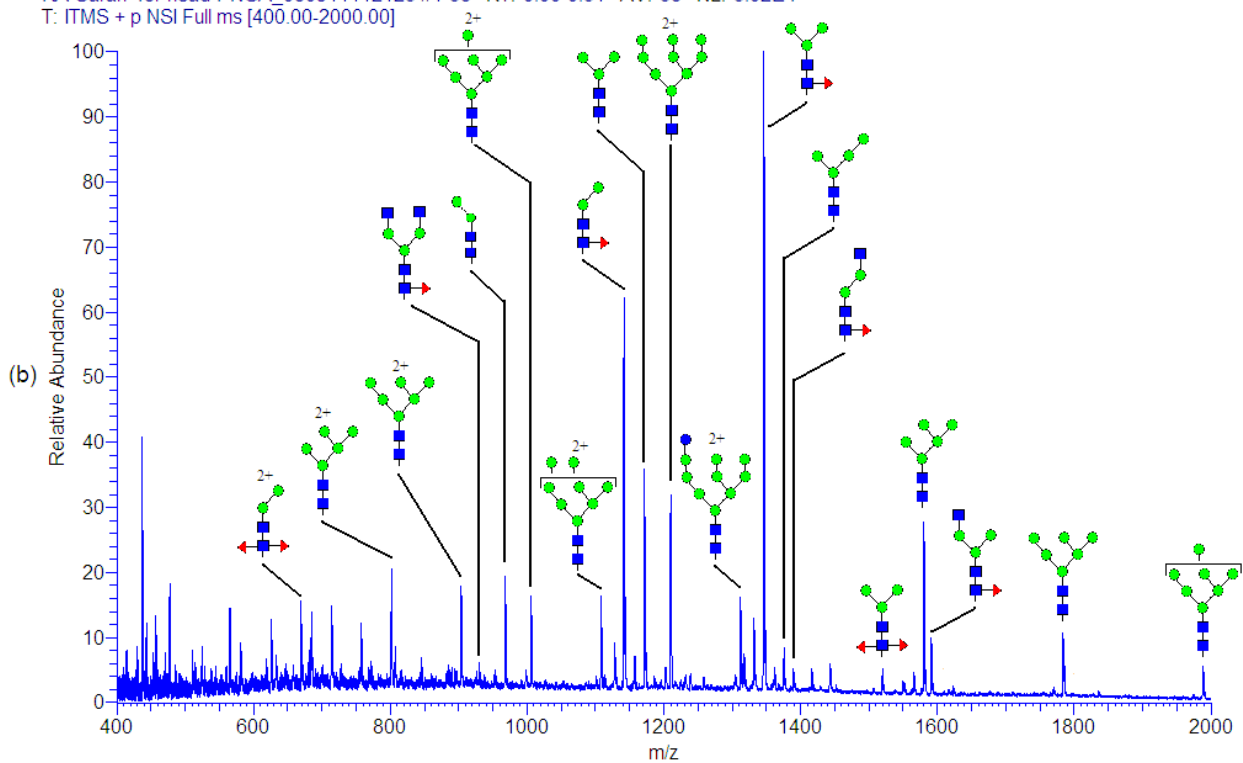


Figure 15. **N-linked glycan profile of OreR and  $w^+$ ; *sff* adult heads.** Total profile for (a) OreR and (b)  $w^+$ ; *sff* adult heads.

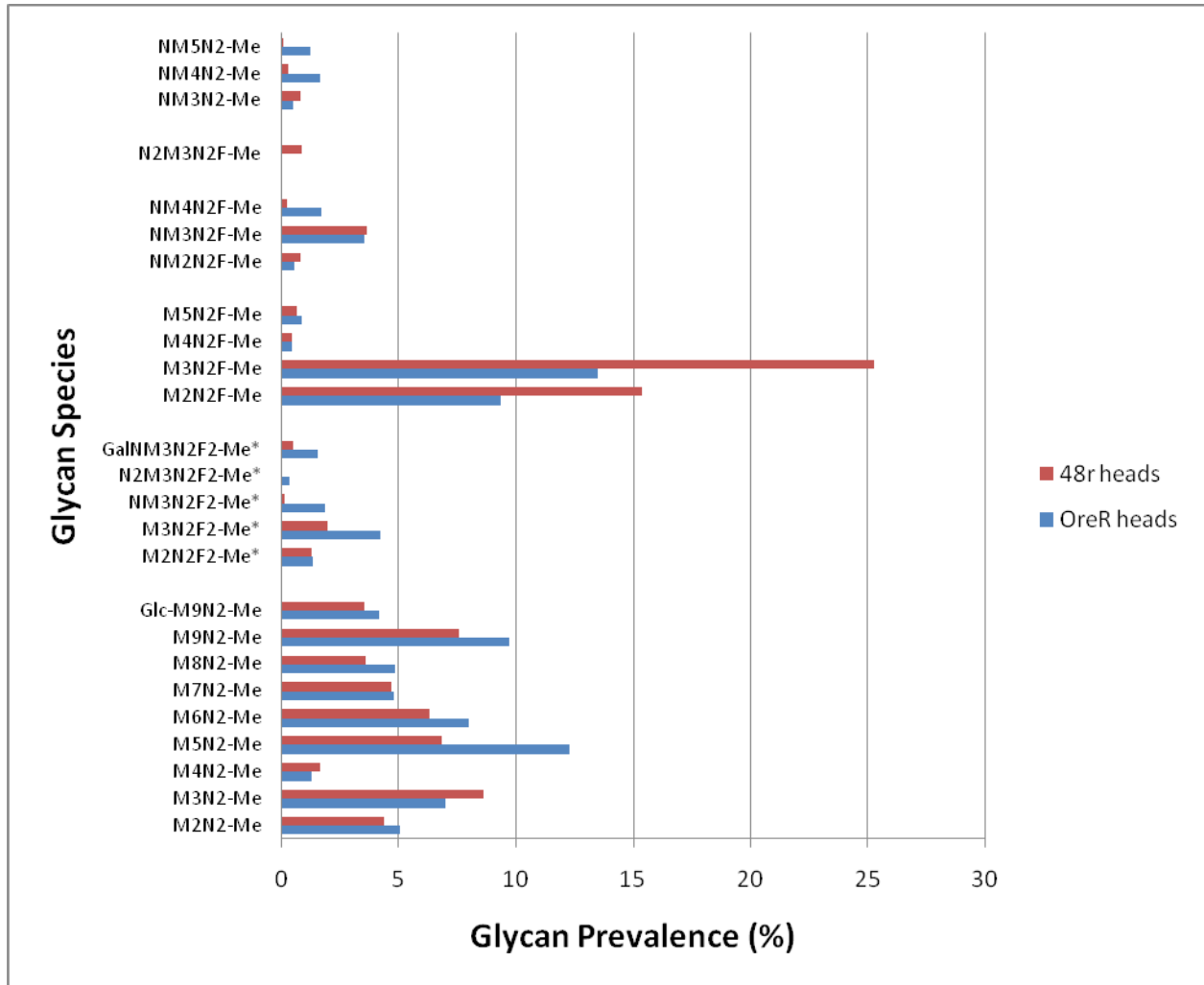


Figure 16. **N-glycan prevalence of OreR and  $w^+$ ; *sff* adult heads.** *sff* adult heads show a decrease in HRP-epitopes(\*) and an increase in monofucosylated structures.



Figure 17. **N-linked glycan profile of  $w^{1118}$  and  $w^+$ ; *sff* larval brains.** Total profile for (a)  $w^{1118}$  and (b)  $w^+$ ; *sff* heads.

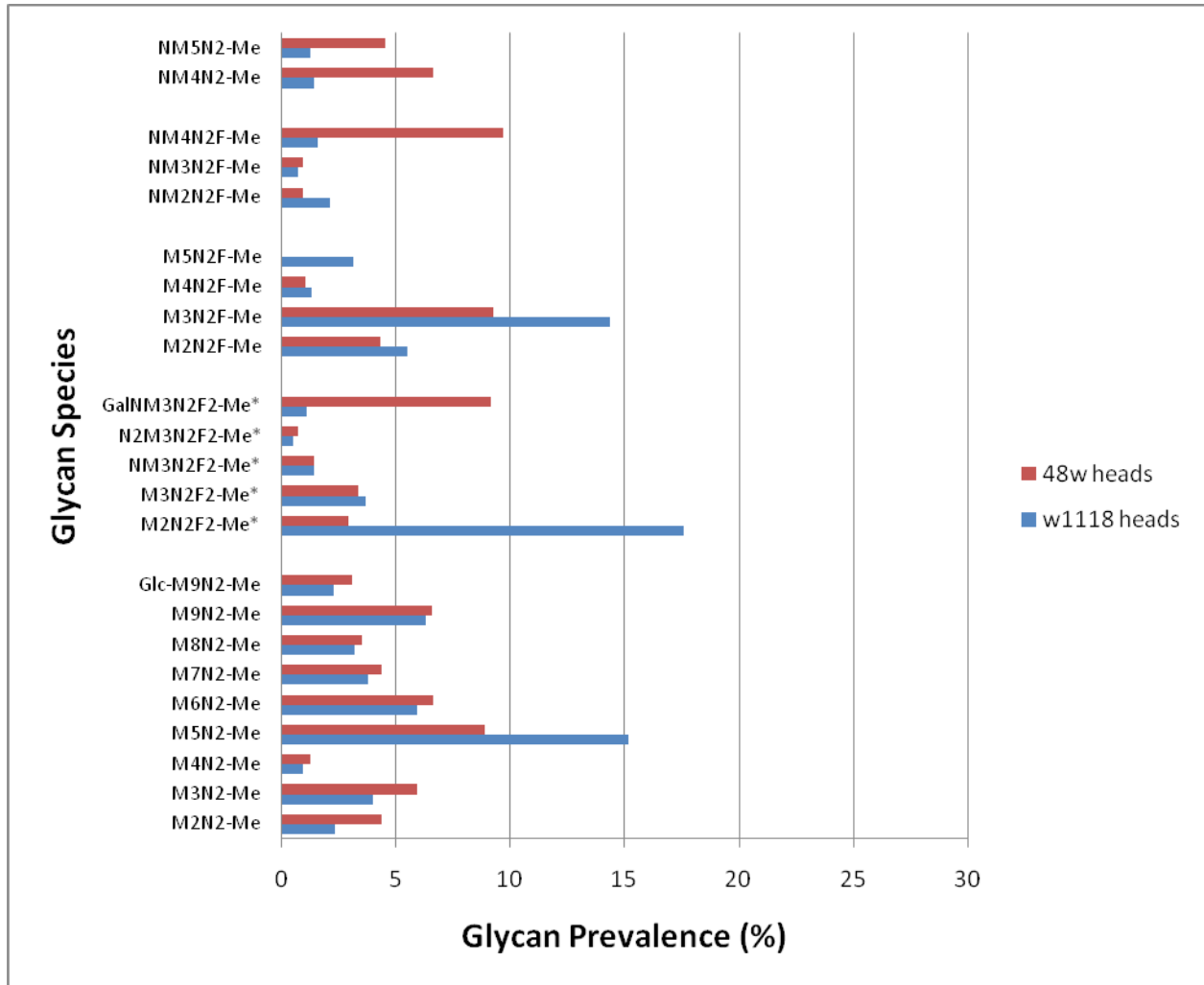


Figure 18. **N-glycan prevalence of  $w^{1118}$  and  $w^+$ ; *sff* adult heads.**  $w^+$ ; *sff* adult heads show a decrease in HRP-epitopes(\*) and an increase in GnT products.

## CHAPTER 5

### GEOTAXIS TESTING OF MUTANTS AND DEVELOPMENT OF GEOTAXIS SCREEN

#### *Geotaxis Behavioral Test*

The results of the geotaxis behavioral testing of MS16-2 and *sff* male flies reveal a definite effect of the decrease in HRP-epitope expression in these two mutants. The control w<sup>1118</sup> flies, for the most part, climbed to the top of the vial within 15 seconds (Figure 19). MS16-2 and *sff* flies, however, do not exhibit this dynamic behavior. In *sff* flies, the behavior is the most severe, as the majority of the flies did not climb to the top within the maximum 120 seconds. Most of the *sff* fly remained at the bottom of the vial and few climb up the vial, exhibiting diminished and restricted movements. In MS16-2 flies, the geotaxis abnormality is not as pervasive as in *sff* flies, but significant enough to distinguish from wild type behavior.

The similarity in the behavioral defect suggests that the *sff* and MS16-2 mutations have the same effect in neurological development. Possibly, the *sff* and MS16-2 mutations affect different components in the same neurological development pathway. Judging from the N-glycans data obtained for MS16-2 and *sff*, it is possible that these mutations alter different components in the N-glycan biosynthetic pathway that result in similar defects in behavior. A good way of discerning the actions of the MS16-2 and *sff* mutation would be to map each mutation and see which gene is mutated.

#### *Development of Geotaxis Screen*

The geotaxis behavioral defects in MS16-2 and *sff* serve as a basis for developing a mutagenesis screen that would screen for mutants that have a similar geotaxis defect. Finding more mutations in geotaxis behavior would hopefully generate mutations that represent alterations in the HRP-epitope biosynthetic pathway. Study of the generated mutants would provide further information into the regulation and mechanism of HRP-epitope synthesis.

Mutants are generated from an ethyl methane sulfonate mutagenesis and put through a screen that tests the geotaxis behavior of the possible mutants (Figure 20). Male  $w^{1118}; D/TM3$  (TM3 is a balancer) flies are fed ethyl methane sulfonate and subsequently mated with  $+$ ; *sff* females. Progeny from the cross that are male  $+$ ; *sff* / TM3 are mated with female OreR (wildtype). The *sff* /  $+$  male progeny from that cross are then put through a geotaxis test. The test involves collecting males and aging them to four days. At four days, the males are starved for four hours in a clear plastic vial at 18°C. After starving the males are given a 15 second window to escape by removing the plug on the vial. The flies that escape within 15 seconds are collected into a bottle that is placed on top of the vial and tested again. The flies that remain are also tested again. The flies that remain twice are kept and mated to female  $+$ ; Kr/CyO. The flies that escape any time during the two trials are thrown away. The males that have been mated are then tested again four days later (males are now at eight days old) using the same method. Again, males that remain twice are kept to continue mating and those that escape are thrown away. From the progeny of the twice-confirmed mutants, 10-20 Kr/CyO male progeny are used to create individual lines by mating them with Kr/CyO females. The male progeny from the individual lines are tested separately to see if they have a geotaxis behavior defect. The males that are

thrice-confirmed mutants should be legitimate mutants that could have defects in HRP-epitope synthesis and the fucosylation pathway.

The geotaxis screen is a useful tool in discovering new mutants in the HRP-epitope synthesis pathway. The screen is an efficient method of screening through mutants and finding those that are similar to MS16-2 and *sff*. The success of the screen would provide an incredible effort towards discovering more about the aspects of the HRP-epitope biosynthetic pathway. Learning more about a relatively unknown pathway that is essential in neural development has many benefits for knowing more about the role of tissue-specific fucosylation in the neural development of not only *Drosophila melanogaster*, but also in humans.

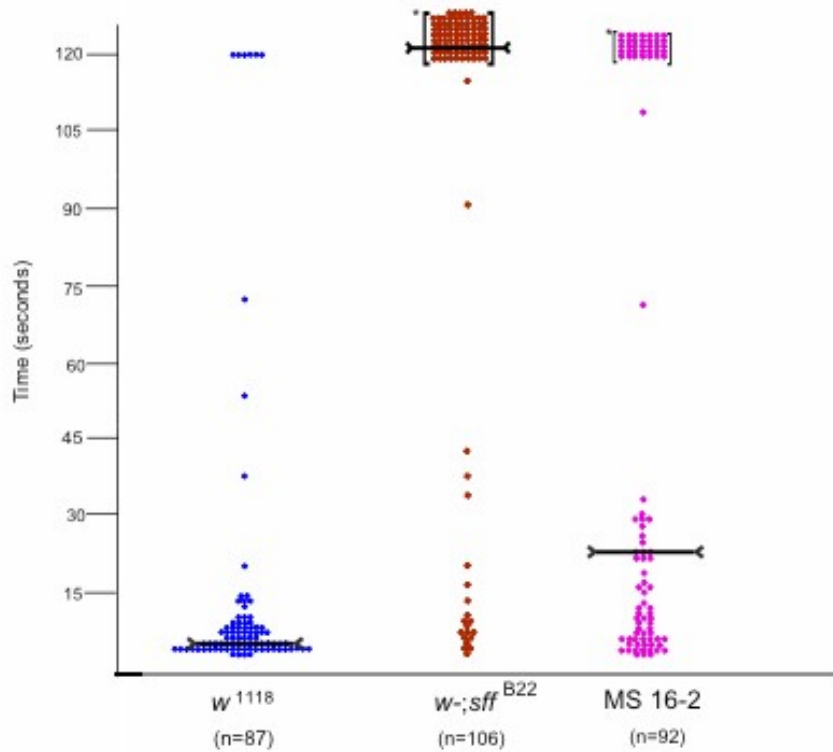


Figure 19. **Geotaxis testing data for  $w^{1118}$ , *sff*, and MS16-2 adult male flies.** The majority of  $w^{1118}$  males escape within 15 seconds. The majority of *sff* males do not escape within the maximum allotted time. MS16-2 males exhibit a substantial deviation from wild type behavior, but not as robust as *sff*. The black line marks the average time for all flies in each phenotype.

## 2nd Chromosome Escape Test Screen

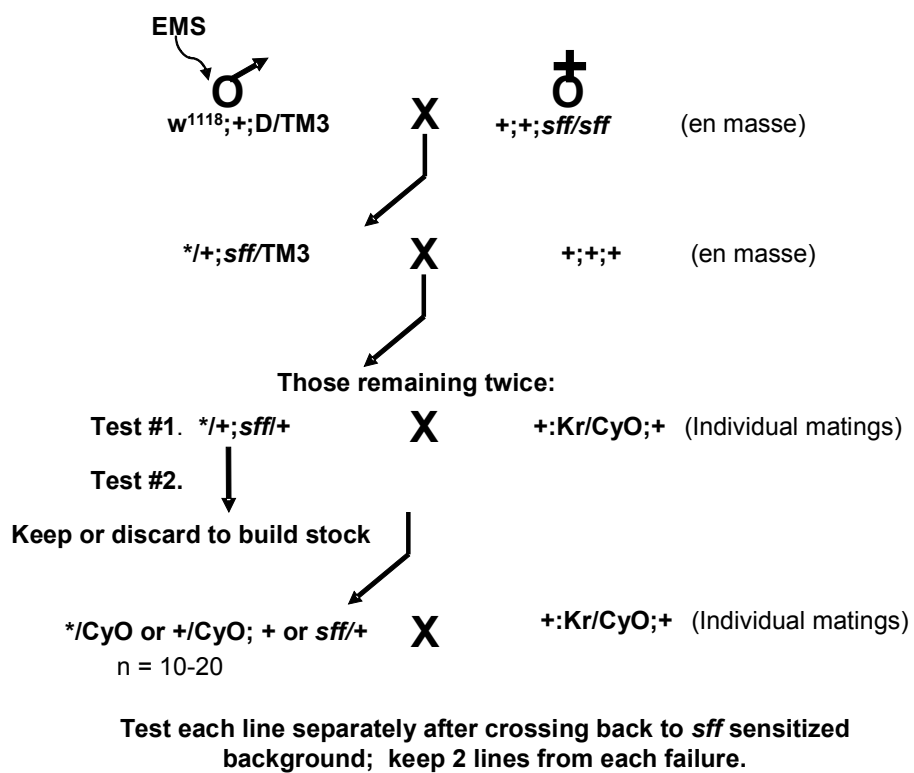


Figure 20. Steps in Geotaxis Screening.

## WORKS CITED

- Seppo, A., Matani, P., Sharrow, M., and Tiemeyer, M. (2003). Induction of neuron specific glycosylation by Tollo/Toll-8, a *Drosophila* Toll-like receptor expressed in non-neural cell. *Development* **130**, 1439-1448.
- Natsuka, S. (2005). Comparative biochemical view of N-glycans. *Trends Glycosci. Glycotechnol.*, **17**, 229-236.
- Aoki, K., Perlman, M., Lim, J., Cantu, R., Wells, L., and Tiemeyer, M. (2007). Dynamic Development Elaboration of N-linked Glycan Complexity in the *Drosophila melanogaster* Embryo. *The Journal of Biological Chemistry*, **282**, 9127-9142.
- Sharrow, M., Rendic, D., Aoki, K., Porterfield, M., Nguyen, K., Overcarsh, B., Kapurch, J., Wilson, I., and Tiemeyer, M. (2008). The balance between O-fucosylation and N-linked core fucosylation influences cell signaling during *Drosophila* development. 2008 Annual Meeting of the Society for Glycobiology, November 12-15, 2008.